JOURNAL OF MATERIALS SCIENCE 20 (1985) 2575–2585

Internal material damping of polymer matrix composites under off-axis loading

C. T. SUN
Department of Engineering Sciences, University of Florida, Gainesville, Florida 32611, USA

R. F. GIBSON
Department of Mechanical Engineering, University of Idaho, Moscow, Idaho 83843, USA

S. K. CHATURVEDI
Department of Engineering Mechanics, University of Missouri-Rolla, Rolla, Missouri 65401, USA

The objective of this paper is to determine theoretically the material damping of short fibre-reinforced polymer matrix composites. The major damping mechanism in such composites is the viscoelastic behaviour of the polymer matrix. The analysis was carried out by developing a finite-element program which is capable of evaluating the stress and strain distribution of short fibre composites under axial loading (see Fig. 1a). Using the concept of balance of force we can express the modulus E_x along the loading direction as a function of the mechanical properties of the fibre and matrix materials, fibre aspect ratio, l/d, loading angle, θ, and fibre volume fraction, V_f. Then we apply the elastic-viscoelastic correspondence principle to replace all the mechanical properties of the composite, fibre and matrix materials such as E_x, E_f, E_m, G_m, by the corresponding complex moduli such as $E'_x + iE''_x$, and $E'_f + iE''_f$. After separation of the real and imaginary parts, we can express E'_x and E''_x as functions of the fibre aspect ratio, l/d, loading angle, θ, stiffness ratio, E_f/E_m, fibre volume fraction, V_f, and damping properties of the fibre and matrix materials such as η_f and η_m. Numerical results of the composite storage modulus, E'_x, loss modulus, E''_x, and loss factor (damping), η_c, are plotted as functions of parameters such as l/d, θ, V_f, and are discussed in terms of variations of l/d, θ, and E_f/E_m, in detail. It is observed that for a given composite, there exist optimum values of l/d and θ at which E''_x and η_c are maximized. The results of this paper can be used to optimize the performance of composite structures.

Nomenclature

A_c, A_f, A_m	cross-sectional area of composite, fibre and matrix, respectively
d	fibre diameter
E_L	longitudinal modulus of composite (along the fibre direction) (see Fig. 1a)
E_T	transverse modulus of composite (see Fig. 1a)
E_x	modulus of composite along the x-direction (see Fig. 1b)
E_f	tensile modulus of fibre
E_m	tensile modulus of matrix
G_m	shear modulus of matrix
G_{LT}	in-plane shear modulus of composite (see Fig. 1a)
l	fibre length
m	tip to tip distance between fibres

0022–2461/85 $03.00 + .12

i	$(-1)^{1/2}$
R	one-half of centre-to-centre fibre spacing
V_f	fibre volume fraction
x	distance along fibre from end of fibre
α	defined in Equation 22
β	defined in Equation 3
β^*	defined in Equation 19
ϵ_L	extensional (longitudinal strain) of composite
ϵ_f, ϵ_m	extensional (longitudinal strain) of fibre and matrix, respectively
η_c, η_f, η_m	extensional loss factor of composite, fibre and matrix respectively
η_{Gm}	shear loss factor of matrix
θ	angle between fibre and the x-direction
$\bar{\sigma}_c$, $\bar{\sigma}_f$, $\bar{\sigma}_m$	average longitudinal stress in composite, fibre and matrix, respectively
σ	longitudinal stress in fibre
τ	shear stress at fibre–matrix interface
ψ	defined in Equation 23

1. Introduction

It is desirable to design a structure with high stiffness, high strength, low weight, low coefficient of thermal expansion, high thermal conductivity and also high damping (or loss modulus). Good damping is extremely important for structures when they are used under dynamic loading environments such as structures used in aerospace applications. The objective of this research is to first derive analytically the loss modulus, E''_x, and storage modulus E'_x as functions of fibre matrix stiffness ratio, E_f/E_m, fibre aspect ratio, l/d, fibre volume fraction, V_f, loading angle, θ (the angle between the fibre direction and the direction of the applied axial force), and the damping properties of the fibre and matrix materials. We then optimize E'_x, E''_x and $\eta_c = E''_x/E'_x$ and obtain optimum values of l/d and θ at which peak values E''_x and η_c occur for a given E_f/E_m.

One of the first papers to report on optimization of damping in structural materials was that of Plunkett and Lee [1]. The damping of basic composite structures was improved by introducing thin constrained viscoelastic layers on the top and bottom of the structures. These viscoelastic layers were stiffened by constraining layers with stiffness equivalent to that of the base structure. Plunkett and Lee presented a method [1] for increasing this damping by cutting the constraining layer into appropriate lengths. Thus, they optimized the damping property of the base structure by using the optimum length of the constraining layer. The analysis was based upon effective complex moduli of an equivalent homogeneous medium.

Experimental investigations have indicated [2, 3] that damping of discontinuous or short fibre-reinforced polymer matrix composites is in general greater than that of continuous fibre-reinforced composites. Gibson *et al.* [4] found the theoretical optimum damping property of discontinuous aligned short fibre composites for the case when the axial load is parallel to the fibre direction. The optimum fibre aspect ratio, l/d, was derived for a given fibre matrix stiffness ratio, E_f/E_m. The analysis was based upon Cox's [5] shear-lag model for determination of the stress distribution along the short fibre. The concept of balance of force and the elastic-viscoelastic correspondence principle were then applied to derive the storage modulus, E'_L, and the loss modulus, E''_L, as functions of such parameters as E_f/E_m, V_f and l/d. In another publication by Sun *et al.* [6], damping of short aligned fibre-reinforced polymer matrix composites was optimized for the case when the fibre direction makes an angle θ with the direction of the applied load. The loss modulus, E''_x, was optimized in terms of l/d as well as the loading angle θ.

This paper is an extension of the research work published in [4, 6]. In Cox's shear-lag model, one important assumption was equal extensional strain in the fibre and matrix materials. Based upon the preliminary investigation by Sun and Wu [7], the assumption of equal extensional strain cannot be justified for the cases (a) high stiffness ratio E_f/E_m, and (b) low volume fraction, V_f. In this investigation we have developed a finite-element program which is capable of determining the stress and strain distribution along a short fibre. We use the finite-element program to modify the Cox's shear-lag model. Then the concept of balance of force and the elastic-viscoelastic correspondence principle are applied to derive E''_x and E'_x as functions of such parameters as E_f/E_m, l/d, θ and V_f. Optimum values of l/d and θ to optimize $\eta_c = E''_x/E'_x$ are obtained. A comparison of the numerical results obtained from Cox's shear-lag model with those

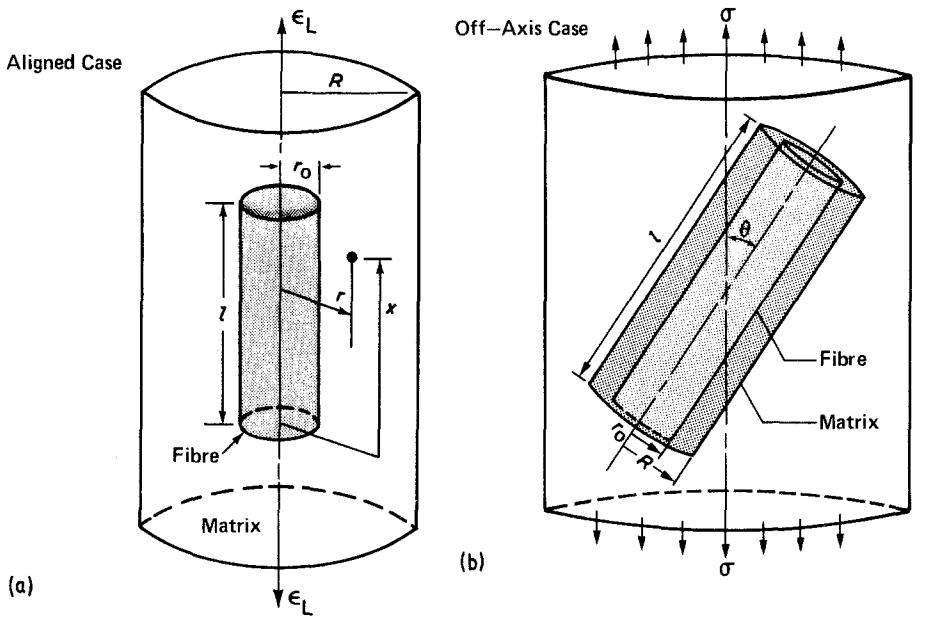

Figure 1 Representative volume element. (a) Aligned case. (b) Off-axis case.

obtained from the finite-element model is also made.

2. Analysis

The analysis has been carried out in [6] in detail. For the sake of continuity, however, the essential part of the development will be presented in this section.

For a typical representative volume element as shown in Fig. 1b the expression of the modulus, E_x, along the loading direction x is given by [8].

$$\frac{1}{E_x} = \frac{\cos^4\theta}{E_L} + \frac{\sin^4\theta}{E_T} + \left(\frac{1}{G_{LT}} - \frac{2\nu_{LT}}{E_L}\right)\sin^2\theta\cos^2\theta \tag{1}$$

Equation 1 was originally derived for continuous fibre reinforced composites. E_L, E_T, G_{LT} and ν_{LT} can be expressed in terms of E_f, E_m, G_f, G_m, etc, and fibre volume fraction, V_f, either from the rules-of-mixtures or the Halpin–Tsai equation [8]. For short aligned fibre composites, however, one cannot use the rule-of-mixtures or Halpin–Tsai equation to represent E_L. For short aligned fibre composites, the longitudinal modulus, E_L, must also depend on the fibre aspect ratio, l/d. Based upon Cox's shear-lag model, E_L is given by [4, 5]

$$E_L = E_f\left(1 - \frac{\tanh\beta l/2}{\beta l/2}\right)V_f + E_m(1 - V_f) \tag{2}$$

where

$$(\beta l)^2 = 8\frac{G_m}{E_f}\frac{(l/d)^2}{\ln(2R/d)^2} \tag{3}$$

In Equation 3 the ratio R/d is related to the fibre volume fraction, V_f, for a specific packing array. For example, for a square packing array

$$\left(\frac{R}{d}\right)^2 = \frac{\pi}{16V_f} \tag{4}$$

and for a hexagonal packing array

$$\left(\frac{R}{d}\right)^2 = \frac{\pi}{8(3V_f)^{1/2}} \tag{5}$$

Based upon a preliminary investigation [4], packing geometry has an insignificant effect on the magnitude of damping or on the optimum aspect ratio, l/d. Therefore we use a square packing array in our subsequent analysis. From Equations 3 and 4 we find that

$$\frac{\pi}{4V_f} \geqslant 1 \tag{6}$$

from which we have

$$V_f \leqslant \frac{\pi}{4} = 0.785 \tag{7}$$

This implies that for square array packing, V_f cannot exceed 78.5%. Otherwise, from Equation 3 $(\beta l)^2$ becomes negative, which is physically impossible.

Substitution of Equation 4 into Equation 3 yields

$$(\beta l)^2 = 16 \frac{G_m}{E_f} \frac{(l/d)^2}{\ln(\pi/4V_f)} \quad (8)$$

Equation 8 shows that the parameter βl is essentially a function of fibre matrix stiffness ratio, E_f/E_m, fibre aspect ratio, l/d, and fibre volume fraction, V_f.

The transverse modulus, E_T, and the in-plane shear modulus, E_T and G_{LT}, are almost independent of fibre aspect ratio, l/d. Therefore, we can use the same formulas as in the case of continuous fibre composites. In this investigation we use Halpin–Tsai equations, i.e.

$$E_T = E_m(1 + 2\eta_1 V_f)(1 - \eta_1 V_f) \quad (9)$$

$$G_{LT} = G_m(1 + \eta_2 V_f)/(1 - \eta_2 V_f) \quad (10)$$

where

$$\eta_1 = [(E_f/E_m) - 1]/[(E_f/E_m) + 2] \quad (11)$$

$$\eta_2 = [(G_f/G_m) - 1]/[(G_f/G_m) + 1] \quad (12)$$

For the major Poissons ratio, ν_{LT}, which is not sensitive to fibre length, we use the rule-of-mixtures, i.e.

$$\nu_{LT} = V_f\nu_f + \nu_m(1 - V_f) \quad (13)$$

In order to determine damping of the composite we assume that both fibre and matrix are viscoelastic materials. This permits us to use the elastic–viscoelastic correspondence principle to redefine the basic material properties as

$$\begin{aligned} E_x &= E_x^* = E_x' + iE_x'' \\ E_f &= E_f^* = E_f' + iE_f'' \\ E_m &= E_m^* = E_m' + iE_m'' \\ G_m &= G_m^* = G_m' + iG_m'' \end{aligned} \quad (14)$$

where prime quantities represent the storage moduli and the double prime quantities represent the loss moduli. Damping (or loss factor) is defined as the ratio between loss modulus to the storage modulus, i.e.

$$\begin{aligned} \eta_c &= E_x''/E_x' \\ \eta_f &= E_f''/E_f' \\ \eta_m &= E_m''/E_m' \\ \eta_{Gm} &= G_m''/G_m' \end{aligned} \quad (15)$$

After using Equation 14, Equations 2, and 8 to 10 can be written as

$$E_L^* = (E_f' + iE_f'')\left(1 - \frac{\tanh\beta^* l/2}{\beta^* l/2}\right)V_f + (E_m' + iE_m'')(1 - V_f) \quad (16)$$

$$E_T^* = (E_m' + iE_m'')\frac{1 + 2\eta_1^* V_f}{1 - \eta_1^* V_f} \quad (17)$$

$$G_{LT}^* = (G_m' + iG_m'')\frac{1 + \eta_2^* V_f}{1 - \eta_2^* V_f} \quad (18)$$

where

$$(\beta^* l)^2 = 16 \frac{G_m'' + iG_m''(l/d)^2}{E_f' + iE_f''\ln(\pi/4V_f)} \quad (19)$$

$$\eta_1^* = \frac{[(E_f' + iE_f'')/(E_m' + iE_m'')] - 1}{[(E_f' + iE_f'')/(E_m' + iE_m'')] + 2} \quad (20)$$

$$\eta_2^* = \frac{[(G_f' + iG_f'')/(G_m' + iG_m'')] - 1}{[(G_f' + iG_f'')/(G_m' + iG_m'')] + 1} \quad (21)$$

Substituting E_L^*, E_T^* and G_{LT}^* from Equations 16 to 18 for E_L, E_T and G_{LT}, respectively, and E_x^* for E_x into Equation 1 we obtain

$$\frac{1}{E_x' + iE_x''} = \frac{\cos^4\theta}{E_L^*} + \frac{\sin^4\theta}{E_T^*} + \left(\frac{1}{G_{LT}^*} - \frac{2\nu_{LT}}{E_L^*}\right)\sin^2\theta\cos^2\theta \quad (22)$$

Equation 22 can be used to determine E_x' and E_x'' for the composites by separating the real and imaginary parts. Since E_L^* is an exponential function of $\beta^* l$ as shown in Equation 16 which depends upon the complex stiffness ratio of G_m^*/E_f^* as indicated in Equation 19, a closed-form expression for the real and imaginary part is very difficult to obtain. The difficulty can be overcome by expanding the exponential term $\tanh\beta^* l$ into power series of the stiffness ratios and then neglecting higher order terms of the loss factors such as η_f^2 and $\eta_f\,\eta_G$ etc. The analytical result is too lengthy to be presented here but it is available in the authors' file. The final result can only be presented in the general form as

$$\begin{aligned} E_x' &= \psi_1(E_m'/E_f', l/d, \theta, V_f, \eta_f, \eta_m, \eta_{Gm}) \\ E_x'' &= \psi_2(E_m'/E_f', l/d, \theta, V_f, \eta_f, \eta_m, \eta_{Gm}) \\ \eta_c &= E_x''/E_x' = \psi_3(E_m'/E_f', l/d, \theta, V_f, \eta_f, \eta_m, \eta_{Gm}) \end{aligned} \quad (23)$$

By assuming all the parameters except one are constants, one can optimize E'_x, E''_x and η_c with respect to that parameter. For example we can optimize η_c with respect to fibre aspect ratio, l/d, from the equation

$$\frac{\partial \psi_3}{\partial (l/d)} = 0 \tag{24}$$

This completes the analysis by using Cox's shear-lag model. Numerical results obtained from this approach are referred to as Cox's shear-lag model results.

As pointed out in Section 1, one of the assumptions "equal extensional strain in the fibre and matrix materials" used in the Cox's analysis [5] cannot be justified. In order to remove this assumption we have developed a finite-element program [7] which is capable of evaluating the stress and strain distribution in the fibre and matrix materials of aligned short fibre composites (Fig. 1a) under axial loading. This finite-element program can be used to modify Equation 2 for E_L.

From the equilibrium equation the average stress in the composite is given by

$$\bar{\sigma}_L = \frac{1}{A_c}\left[\int_{A_f} \sigma_f dA_f + \int_{A_m} \sigma_m dA_m\right] \tag{25}$$

or

$$\bar{\sigma}_L = \bar{\sigma}_f V_f + \bar{\sigma}_m (1 - V_f) \tag{26}$$

where the average stresses $\bar{\sigma}_f$ and $\bar{\sigma}_m$ in the fibre and matrix are, respectively, given by

$$\bar{\sigma}_f = \frac{1}{A_f}\int_{A_f} \sigma_f dA_f = \frac{2}{l}\int_0^{l/2} \sigma_f dx \tag{27}$$

$$\bar{\sigma}_m = \frac{1}{A_m}\int_{A_m} \sigma_m dA_m$$

where

$$V_f = A_f/A_c \text{ and } 1 - V_f = A_m/A_c \tag{28}$$

From Cox's analysis [5] we can obtain

$$\sigma_f = \epsilon_f E_f\left[1 - \frac{\cosh\beta(l/2 - x)}{\cosh\beta l/2}\right] \tag{29}$$

Substituting Equation 28 into the first equation of Equation 27 we obtain

$$\bar{\sigma}_f = \epsilon_f E_f\left[1 - \frac{\tanh\beta l/2}{\beta l/2}\right] \tag{30}$$

The average stresses in the matrix, $\bar{\sigma}_m$, and in the composite, $\bar{\sigma}_L$, can be expressed in terms of ϵ_m and ϵ_c, respectively

$$\bar{\sigma}_m = \epsilon_m E_m \tag{31}$$
$$\bar{\sigma}_L = \epsilon_L E_L$$

Substituting Equations 29 and 30 into the equilibrium Equation 25 we obtain

$$E_m \epsilon_L = E_f \epsilon_f\left(1 - \frac{\tanh\beta l/2}{\beta l/2}\right)V_f + E_m \epsilon_m (1 - V_f) \tag{32}$$

Equation 32 is similar to Equation 2 with the exception that each term is multiplied by the corresponding strain term. With the assumption of equal extensional strain Equation 32 is reduced to Equation 2.

In order to improve analytical results, Equation 32 is still valid since it is derived from equilibrium equation and the one dimensional Hooke's Law. The finite-element program of Sun and Wu [7] which is capable of calculating the strain distribution at every point, can now be used. The detail of development of the program can be found in [7]. Based upon the finite-element program we can determine ϵ_f at a finite number of points at the fibre and ϵ_m in finite number of points in the matrix under a given extensional strain, ϵ_L. Now we can determine the average extensional strains in the fibre and in the matrix, respectively, and express in terms of the extensional strain, ϵ_L, in the following expression

$$\epsilon_f = \alpha \epsilon_L$$
$$\epsilon_m = \gamma \epsilon_L \tag{33}$$

where α and γ are determined numerically from the finite-element program in [7]. Since, in general, ϵ_m is greater than ϵ_f, γ should be greater than unity and α should be less than unity. Substituting Equation 33 into Equation 32 one obtains

$$E_L = E_f\left(1 - \frac{\tanh\beta l/2}{\beta l/2}\right)V_f \alpha + E_m (1 - V_f)\gamma \tag{34}$$

Equation 33 and the corresponding equation

$$E_L^* = (E'_f + iE''_f)\left(1 - \frac{\tanh\beta l/2}{\beta^* l/2}\right)V_f \alpha + (E'_m + iE''_m)(1 - V_f)\gamma \tag{35}$$

should be used to replace Equation 2 and Equation 16, respectively. All the other equations will remain unchanged. The loss modulus E''_x and the

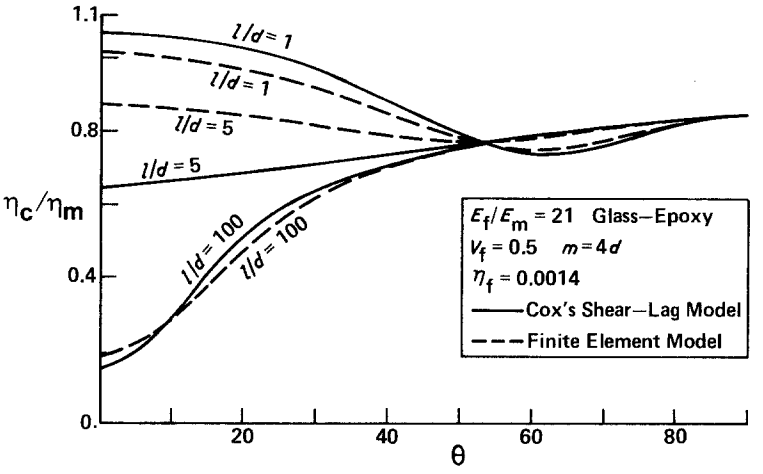

Figure 2 Plot of η_c as a function of θ using l/d as a parameter for glass–epoxy composite.

storage modulus E'_x can be evaluated and optimized by exactly the same procedures. Numerical results obtained this way are referred to as the finite-element model results.

3. Numerical results and discussion

η_c is defined as the ratio of E''_x/E'_x and since both E''_x and E'_x are functions of E_f/E_m, l/d, θ, V_f and η_f etc, the variations of η_c and E''_x may not follow the same pattern. Therefore, in the numerical presentations we have three dependent variables the non-dimensional ratio E'_x/E'_m, the non-dimensional ratio E''_x/E''_m, and the non-dimensional ratio η_c/η_m. In general, we have seven independent variables, namely E_f/E_m, l/d, θ, V_f, η_f, η_m and η_{Gm}. A cross-plot including all the possible variations of the seven variables is almost impossible and unnecessary. In the following we first limit our presentation to epoxy matrix material and four fibre materials; glass, Kevlar, graphite and boron. Also for most composite materials used in aerospace industry the fibre volume fraction varies in a narrow range, from 50% to 60%, so we use $V_f = 50\%$ in the numerical calculation. For an epoxy matrix material we use $\eta_m = 0.015$ and $\eta_{Gm} = 0.018$ [4]. From the above discussion, the active independent variables are now narrowed down fo four; l/d, θ, η_f and four values E_f/E_m.

Fig. 2 presents the non-dimensional loss factor ratio η_c/η_m of glass-epoxy composites as a function of θ using l/d as a parameter. It is interesting to observe that η_c becomes maximum either when $\theta = 0°$ or when $\theta = 90°$. For smaller l/d (say $l/d < 5$) maximum η_c occurs at $\theta = 0°$ and for large l/d the maximum η_c occurs at $\theta = 90°$. This result is in contrast with the relation between E''_x and θ in which the peak values of E''_x occur at some angle of θ other than 0° and 90° for small l/d [6]. It is also observed that the difference in prediction between finite-element model and Cox's shear-lag model becomes significant for small θ and small l/d. The above observations are also valid for boron–epoxy, graphite–epoxy, and Kevlar–epoxy composites.

It is well-known [9] that graphite fibres themselves are orthotropic (i.e. for graphite fibres $E_L \neq E_T$ and the isotropic relation $E = 2(1 + \nu)G$ cannot be satisfied.) In order to take into account the effect of orthotropic fibres, we use the method recommended by Whitney [10]. We denote E_{f1} as the modulus of graphite along the fibre direction and E_{f2} as the modulus of graphite transverse to the fibre direction. In Equations 34 and 16 for E^*_L we use E'_{f1} and E''_{f1} for E'_f and E''_f, respectively, and in Equations 17 and 20 for E^*_T we simply use E'_{f2} and E''_{f2} for E'_f and E''_f, respectively. Numerical results for graphite-epoxy composites are presented in Figs. 3 and 4.

In Fig. 3 we plot η_c/η_m as a function of θ for graphite–epoxy and Kevlar–epoxy composites. We note that η_c/η_m increases as E_f/E_m increases. This result indicates the advantage of using higher modulus fibres. For graphite–epoxy composites, we observe that the inherent orthotropic property of carbon fibres makes a significant difference in predicting η_c for the case when $\theta \geqslant 10°$. This difference increases as θ increases.

In Fig. 4 we plot η_c/η_m for graphite–epoxy and Kevlar–epoxy composites as a function of l/d. For the graphite–epoxy composite, we also examine the effect of orthotropic fibre on η_c. The difference is important only in the region of small l/d. We also examine the difference

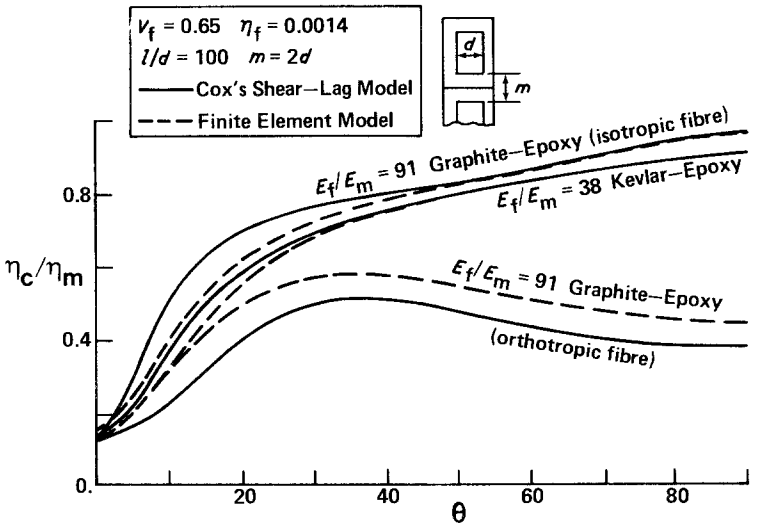

Figure 3 Plot of η_c as a function of θ for different composite materials.

between finite-element and Cox's shear-lag models. Again, significant difference is found only in the region of small l/d.

Fig. 5 shows η_c/η_m for glass–epoxy and boron–epoxy composites as a function of l/d for different values of θ. With the exception of small l/d (say $l/d < 5$), η_c/η_m increases as θ increases. As $\theta \geqslant 60°$, η_c/η_m is almost indepen-

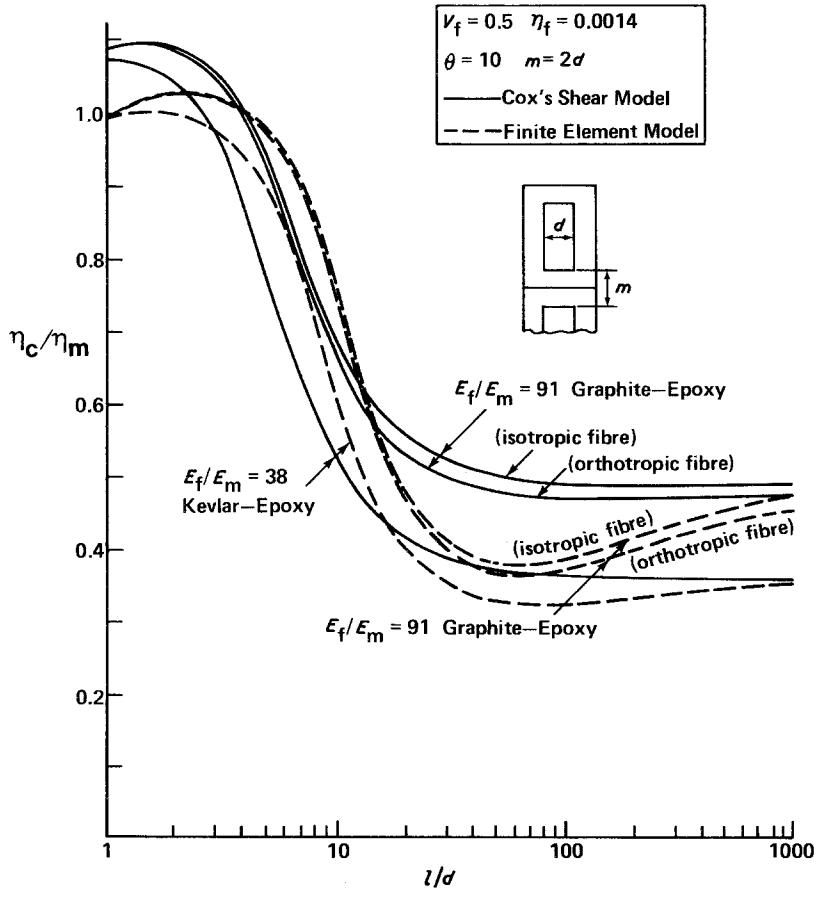

Figure 4 Plot of η_c as a function of l/d for different composite materials.

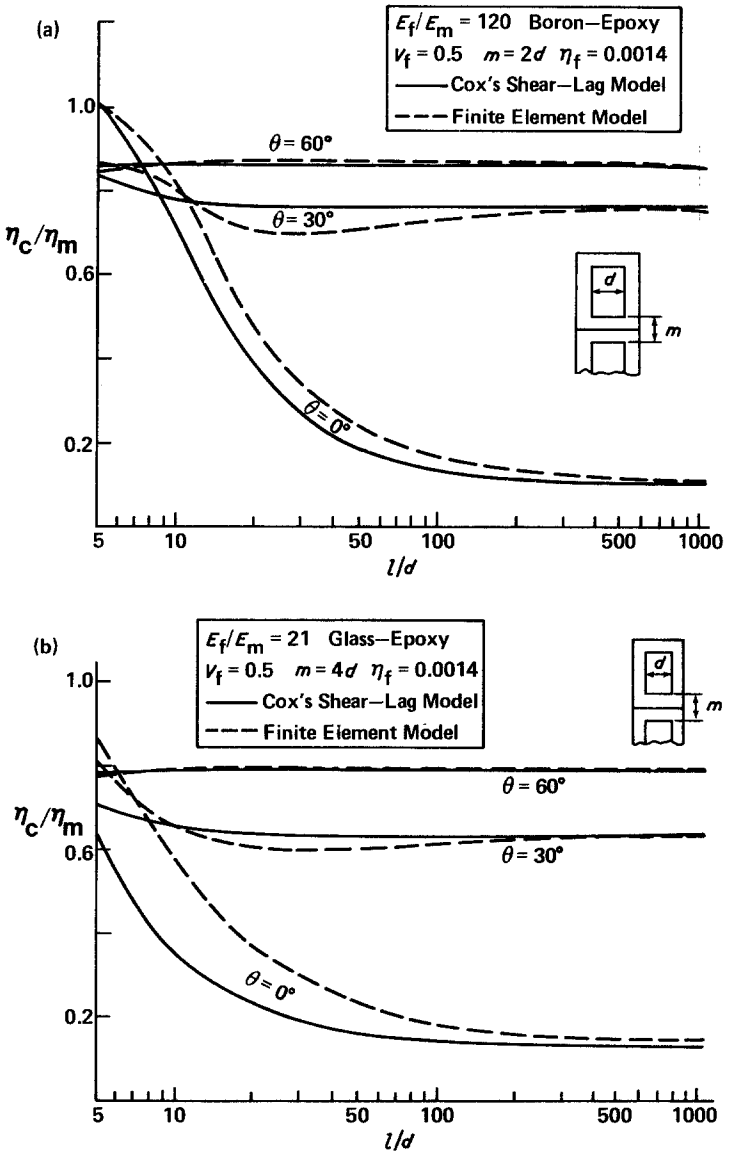

Figure 5 Comparison between finite element model and Cox's shear-lag model – I.

dent of l/d. The difference between the finite-element model and Cox's shear-lag model becomes important again in the region of small θ and small l/d. In Figs. 6 to 8, we plot the non-dimensional E'_x, E''_x and η_c in the same diagram using both finite-element and Cox's shear-lag models. Fig. 6a shows E'_x, E''_x and η_c as a function of θ for large l/d ($l/d = 100$). We first observe that variations of E''_x and η_c do not follow the same pattern. As expected the minimum value of E'_x occurs at $\theta = 0°$ and the maximum η_c occur at $\theta = 90°$. The peak value of E''_x however, occurs at θ near 20°. The predictions of the two models differ significantly for E'_x in the region of small θ (say $0 \leqslant \theta$ 15°). Fig. 6b shows a similar plot for small l/d ($l/d = 10$). For small l/d, the difference in prediction of E'_x, E''_x and η_c by the two models becomes larger in the small θ region than the corresponding difference for large l/d.

Figs. 7 and 8 show plots of E'_x, E''_x and η_c as a function of θ for boron–epoxy composites with two different fibre aspect ratios ($l/d = 10$ in Fig. 7 and $l/d = 100$ in Fig. 8). All the observations in Fig. 6 for glass–epoxy composites are valid for boron–epoxy composites. For boron–epoxy composites (with $E_f/E_m = 120$) however, the difference between the two models in prediction of E'_x, E''_x and η_c is greater than the corresponding prediction for glass–epoxy composite (with $E_f/E_m = 21$).

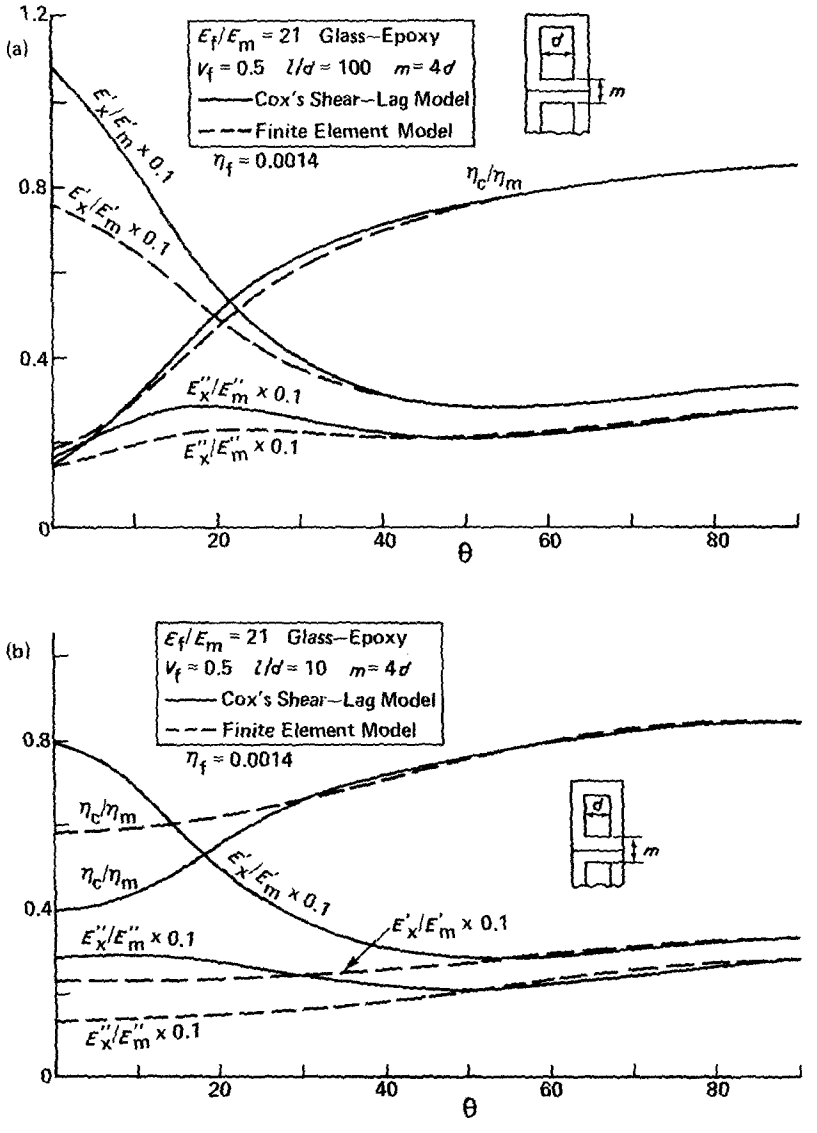

Figure 6 Comparison between finite element model and Cox's shear-lag model – II.

4. Concluding remarks and recommendations

Based upon the results of this paper and [6], we can draw the following conclusions and recommendations regarding optimization of composite structures:

(1) The storage modulus E'_x: (a) for a given l/d, E'_x is maximum at $\theta = 0$ and then decreases as θ increases; (b) for a given θ, E'_x increases asymptotically as l/d goes to infinity; (c) E'_x increases as E_f/E_m and/or V_f increase.

(2) the loss factor $\eta_c = E''_x/E'_x$: (a) for very small l/d (say $l/d < 5$, i.e. in whisker or microfibre range), the maximum η_c occurs for small angles, θ; (b) for large l/d, the maximum η_c occurs at large values of θ; (c) η_c increases as E_f/E_m increases; (d) η_c becomes independent of l/d for large angle of θ (say $\theta > 60°$ and/or large l/d (say $l/d \geqslant 100$).

(3) The loss modulus E''_x: in general the variation of E''_x is more complex than η_c and E'_x. The following observations have been made. (a) For a given E_f/E_m, there exists an optimum fibre aspect ratio, l/d, at which E''_x becomes maximum. (b) Both the peak values of E''_x and the optimum fibre aspect ratio l/d increase significantly when high modulus fibres E_f/E_m are used. Consequently boron, graphite and Kevlar fibres have distinct advantages. (c) For a given E_f/E_m there exists an optimum angle θ at which E''_x becomes

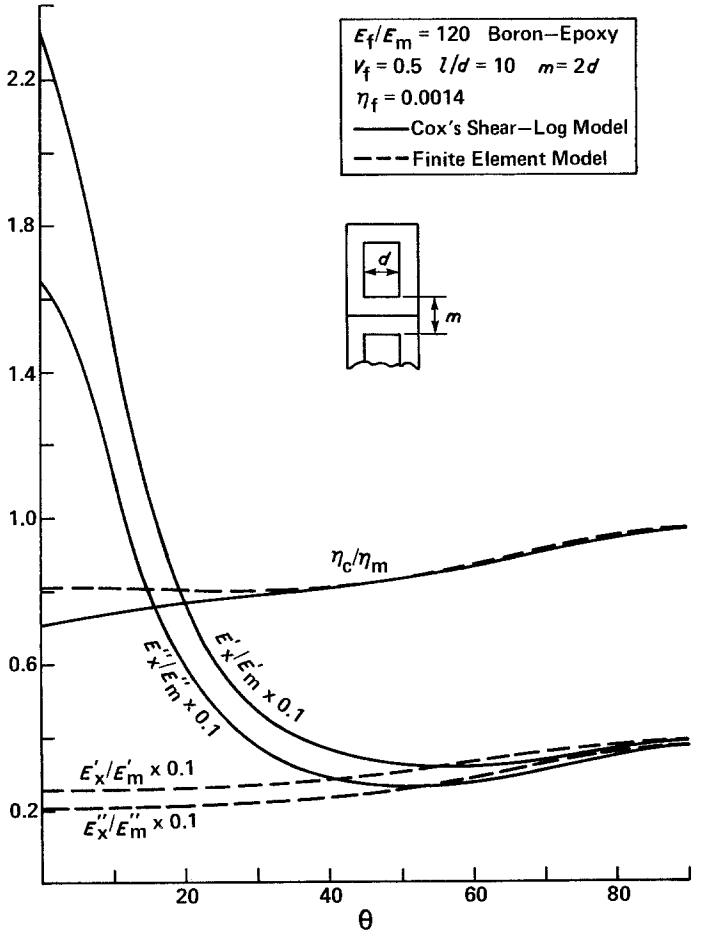

Figure 7 Comparison between finite element model and Cox's shear-lag model – III.

maximum. (d) This optimum angle, θ, decreases as E_f/E_m increases. (e) The peak value of E''_x diminishes as l/d becomes large (say $l/d \geqslant 100$). (f) The influence of θ and l/d on E''_x diminishes when θ is greater than 60°. When $\theta = 90°$, E''_x reaches the same value for all values of l/d. (g) The influence of fibre damping, η_f, on the optimum fibre aspect ratio, l/d, and the optimum angle θ is significant. For relatively large values of η_f (say $\eta_f \geqslant 0.2\ \eta_m$) the optimum fibre aspect ratio, l/d, is in the continuous fibre range (say $l/d \geqslant 100$), and the optimum angle θ is relatively large. For small values of η_f (say $0 \leqslant \eta_f < 0.2\ \eta_m$) the optimum fibre aspect ratio, l/d, is small (say $l/d < 50$), and the optimum angle θ is also small (say $0 \leqslant \theta \leqslant 20°$). ($\eta_m$ is the damping of matrix material.)

(4) Comparison between the Cox's shear-lag model and finite-element model. The difference between the Cox's shear-lag model and finite-element model in predicting E'_x, E''_x and η_c is significant under any one or the combination of the following four conditions. (a) Small loading angle θ (say $\theta \leqslant 30°$). (b) Small fibre aspect ratio l/d (say $l/d \leqslant 50$). (c) Small fibre volume fraction V_f (say $V_f \leqslant 30\%$). (d) Large E_f/E_m.

The most ideal situation for designers designing a structure is to optimize E'_x and E''_x (or η_c) at the same time. Unfortunately, based upon the analytical research shown here we cannot optimize both E'_x and E''_x simultaneously. The situation between E'_x and η_c is, however, slightly different. The analytical results show that for small loading angles θ (say $\theta \leqslant 30°$), η_c becomes maximum in the whisker or microfibre composites range (i.e. very small l/d, say $l/d \leqslant 5$). The stiffness E'_x for microfibre and whisker composites is also relatively high. Therefore, in order to achieve high stiffness E'_x and high damping η_c, microfibre and whisker composites seem to be the ideal candidates.

The second possible means of achieving high stiffness and high damping of a composite is to choose fibres with relatively large damping.

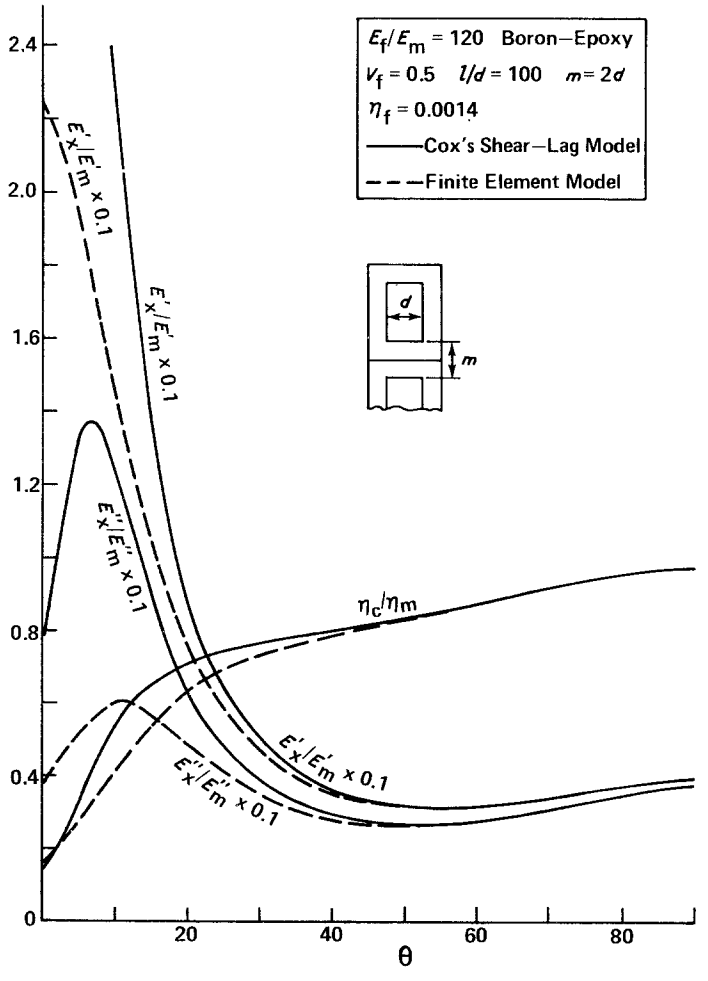

Figure 8 Comparison between finite element model and Cox's shear-lag model – IV.

Kevlar fibres are known to have such a property. Therefore, in order to achieve high stiffness and high damping, Kevlar, microfibre, and whisker composites are recommended. In general, if we use other fibres such as boron and graphite, a trade-off must be made in order to optimize structural performance.

Acknowledgement

The authors gratefully acknowledge support of this research work from Air Force Office of Scientific Research under Grant No. AFOSR-83-0154 monitored by Dr D. R. Ulrich, Program Manager, Directorate of Chemical and Atmospheric Sciences AFOSR, Bolling Air Force Base, Washington, DC.

References

1. R. PLUNKETT and C. T. LEE, *J. Acoustical Soc. Amer.* **48** (1970) 159.
2. D. McLEAN and B. E. REED, *J. Mater. Sci.* **10** (1975) 481.
3. R. F. GIBSON and A. YAU, *J. Compos. Mater.* **14** (1980) 155.
4. R. F. GIBSON, S. K. CHATURVEDI and C. T. SUN, *J. Mater. Sci.* **17** (1982) 3499.
5. H. L. COX, *Brit. J. Appl. Phys.* **3** (1952) 72.
6. C. T. SUN, S. K. CHATURVEDI and R. F. GIBSON, *J. Computer and Structures*, January (1985) p. 285.
7. C. T. SUN and J. K. WU, *J. Reinforced Plastics Composites* **3** (1984) 130.
8. B. D. AGARWAL and L. J. BROUTMAN, "Analysis and Performance of Fibre Composites" (Wiley Interscience, New York, 1980) p. 125.
9. J. E. ASHTON, J. C. HALPIN and P. H. PETIT, "Primer on Composite Materials; Analysis" (Technomic Publications, Stanford, Connecticut, 1969) p. 113.
10. J. M. WHITNEY, *J. Compos. Mater.* **1** (1967) 188.

Received 25 June
and accepted 20 September 1984